

This is the peer reviewed version of the following article:


Interfacial shear stress analysis of bar and thin film bonded to 2D elastic substrate using a coupled FE-BIE method / Tullini, Nerio; Tralli, Antonio; Lanzoni, Luca. - In: FINITE ELEMENTS IN ANALYSIS AND DESIGN. - ISSN 0168-874X. - 55:(2012), pp. 42-51. [10.1016/j.finel.2012.02.006]

Terms of use:

The terms and conditions for the reuse of this version of the manuscript are specified in the publishing policy. For all terms of use and more information see the publisher's website.

19/12/2025 03:00

AUTHOR QUERY FORM

	Journal: FINEL Article Number: 2659	Please e-mail or fax your responses and any corrections to: E-mail: corrections.esch@elsevier.macipd.com Fax: +44 1392 285878
---	--	--

Dear Author,

Please check your proof carefully and mark all corrections at the appropriate place in the proof (e.g., by using on-screen annotation in the PDF file) or compile them in a separate list. Note: if you opt to annotate the file with software other than Adobe Reader then please also highlight the appropriate place in the PDF file. To ensure fast publication of your paper please return your corrections within 48 hours.

For correction or revision of any artwork, please consult <http://www.elsevier.com/artworkinstructions>.

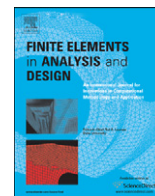
Any queries or remarks that have arisen during the processing of your manuscript are listed below and highlighted by flags in the proof. Click on the [Q](#) link to go to the location in the proof.

Location in article	Query / Remark: click on the Q link to go Please insert your reply or correction at the corresponding line in the proof
Q1	Please confirm that given names and surnames have been identified correctly.

Thank you for your assistance.

Contents lists available at [SciVerse ScienceDirect](#)

Finite Elements in Analysis and Design

journal homepage: www.elsevier.com/locate/finel

Highlights

Interfacial shear stress analysis of bar and thin film bonded to 2D elastic substrate using a coupled FE–BIE method

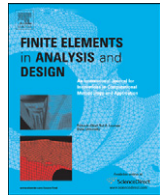
Nerio Tullini^a, Antonio Tralli^a, Luca Lanzoni^b^a Department of Engineering, University of Ferrara, Italy^b Dipartimento di Ingegneria Meccanica e Civile, University of Modena and Reggio Emilia, Italy

► Elastic thin structures bonded to a half-plane under axial forces or thermal loads are considered. ► A coupled FE–BIE method is proposed to evaluate the mechanical behaviour. ► Accurate evaluations of shear stress singularity factors are given.

Finite Elements in Analysis and Design ■ (■■■■) ■■■–■■■

Contents lists available at [SciVerse ScienceDirect](http://SciVerse.ScienceDirect)

Finite Elements in Analysis and Design

journal homepage: www.elsevier.com/locate/finel

Interfacial shear stress analysis of bar and thin film bonded to 2D elastic substrate using a coupled FE–BIE method

Q1 Nerio Tullini^{a,*}, Antonio Tralli^a, Luca Lanzoni^b^a Department of Engineering, University of Ferrara, Italy^b Dipartimento di Ingegneria Meccanica e Civile, University of Modena and Reggio Emilia, Italy

ARTICLE INFO

Article history:

Received 10 September 2011

Received in revised form

22 February 2012

Accepted 23 February 2012

Keywords:

Thin film–substrate interaction

Mixed finite elements

Interfacial shear stress

Shear stress singularity factor

Green function

ABSTRACT

In the present work, a Finite Element–Boundary Integral Equation (FE–BIE) coupling method is proposed to investigate the problem of axially loaded thin structures bonded to a homogeneous elastic half-plane. Making use of a mixed variational formulation including the Green function of the substrate, the axial displacement of the bar is interpolated using Lagrange polynomials of first or second order, whereas the interfacial shear stress is approximated by piecewise constant functions. Bars subject to different load conditions are investigated, including the case of a bar partially detached from the substrate. The strength of interfacial stress singularities is investigated in detail.

© 2012 Published by Elsevier B.V.

1. Introduction

The problem of an axially loaded bar attached to a plate has been widely investigated in mechanical and civil engineering, where it is relevant to stress distribution in stiffened sheet [1]. Moreover, interest in the problem has been renewed by composite materials used in structural strengthening of concrete, steel, wood [2], ceramic coatings protecting alloy substrate [3] and electronic devices with metal films bonded to a polymer or silicon substrate [4]. A proper mechanical model of thin film–substrate structures should be adopted to evaluate stress concentrations and strain localizations. Analysis of the stress singularity at the edge is important to evaluate the initiation of the delamination between the film and substrate. The assessment of these local effects is needed to properly design a wide range of electronic devices and micro-components which are typically subject to high stress levels and, in turn, to damaging phenomena like fractures, failures and crack formation and growth. To study stiffener reinforcing thin plates, generalised plane stress state and bar model are often assumed [5–10]. Conversely, plane strain state and membrane model are well-suited to thin films bonded to a substrate [11–15].

The earliest classical study on plates reinforced with stiffeners appears to have been initiated by Melan who analysed an infinite

rib welded to the boundary of an elastic half-plane and loaded by an axial force [5]. Melan obtained an analytical solution of the problem and found a logarithmic growth of interfacial shear stress in the neighbourhood of the load application point, whereas the elastic half-plane loaded by a point force tangential to its boundary is characterised by a square-root singularity, as predicted by the Cerruti solution [16]. Nevertheless, this type of singularity was found later by Buell [6] and Koiter [7] near the stiffener edge of a semi-infinite bar bonded to a semi-infinite plate and loaded by a point force at the end. The problem of a bar of finite length bonded to an elastic half-space and subject to various load conditions was investigated, for example, in [8–10]. In these references, the governing integro-differential equation is solved by adopting power or Chebyshev polynomials series expansion to approximate the unknown interfacial stress. In [11] the stress induced in a semi-infinite elastic substrate by a bonded thin film is studied solving the integral equation via the finite difference method. The author adopted a length of the grid elements varying along the longitudinal direction according to an exponential law, in order to accurately evaluate the substrate reaction, particularly near the film edge.

The finite element (FE) method was extensively adopted in solving problems concerning layered systems because of its potential in simulating complex geometries and various loading conditions. For instance, numerical computations based on FE method were performed in [17] to evaluate stress distribution, strain energy release rates and stress intensities in residual stressed film–substrate systems. FE analyses were developed in [18] to

* Corresponding author.

E-mail addresses: nerio.tullini@unife.it (N. Tullini), tra@unife.it (A. Tralli), luca.lanzoni@unimore.it (L. Lanzoni).

assess the contact stress in single, double-layer and multilayered coated systems subject to a **Hertzian** pressure distribution acting on a portion of the boundary. In [19,20], both normal and tangential load distributions are taken into account in order to simulate interfacial friction effects. In [21] the stress distribution in the substrate underlying the film was investigated by means of the conventional FE method. In [12,13] FE programs were used to evaluate interfacial and axial film stress, respectively, comparing the results with those provided by some analytical models. A conventional FE package was also used in [14] to predict the cracking phenomenon in thin **film-interlayer-substrate** systems subjected to tensile loading. In this reference, interface elements **characterised** by a bilinear constitutive law are adopted in order to predict the distribution of crack spacing in the film.

However, the application of the FE method to thin **film-substrate** systems finds some limitations in simulating layers with very different **thicknesses** [22]. Indeed, various kinds of electronic devices involve film having thickness of the order of some hundreds of nanometres, whereas the substrate thickness typically equals some hundreds of **micrometres** or more. Moreover, it should be noted that the FE meshes near the **film-substrate** interface and in the region close to film edges must be refined to avoid the mesh size effect on the magnitude of the interfacial stresses.

Boundary element (BE) method and boundary integral equation (BIE) were also adopted to study layered systems. In particular, BE technique based on elasticity theory can be used to evaluate in a very efficient and accurate manner the mechanical behaviour of coated systems involving thin layers, as long as the nearly-singular integrals existing in the BE formulations are handled correctly [22–24]. In [25,26] a BE method with fundamental solution for dissimilar materials is used in the thermo-elastic analysis of interfacial stress and stress singularity between a thin film and its substrate.

In the present work, the problem of axially loaded thin structures bonded to a homogeneous isotropic half-plane is studied by means of a **FE-BIE** coupling method. Thin bonded structures are properly treated using bar FEs, without resorting to 2D thin structures, and BIE are restricted to the substrate only. Hence, the relation between bar displacement and interfacial stress involves the Green function of the substrate. Plane strain or **generalised** plane stress condition for the **bar-substrate** system is assumed. Using the theorem of work and energy for exterior domains, a mixed variational formulation is **utilised**, with variational functions represented by bar displacement and interfacial shear stress. In the proposed model, independent partition of bar and underlying substrate can be used, and finite element mesh involves the bar length only. Lagrange polynomials of first or second order are adopted as interpolating functions of the displacement field, whereas interfacial shear stress is described through piecewise constant function. Mixed variational principle, similar to the one presented in this paper, was used in [27] to study the frictionless interaction of a Timoshenko beam with the underlying soil. In this respect, the present work represents the natural extension of the method to analyse a bar, with zero bending stiffness, perfectly bonded to a substrate.

The interaction between an elastic bar and the underlying half-plane is investigated in detail. The case of a bar loaded at the midpoint by a horizontal force of magnitude P is treated first. The response of the system is in terms of axial displacement, axial force and substrate reaction, varying the rigidity parameter of the bar. In particular, the strength of the interfacial stress singularity is evaluated and discussed for this and other load conditions. Comparison of the results furnished by the present model with some classical solutions is given. Finally, the case of a partially detached bar subject to a concentrated force or uniform thermal variation is also considered.

It is worth **noting** that, in the proposed method, the weakly singular BIE is evaluated analytically, avoiding **handling of** singular and hyper-singular integrals, that are the major concern of the classical BE methods. Moreover, the dimension of the resolving matrix is proportional to the number of bar FEs, unlike the classical FE methods where a refined mesh requires a stiffness matrix with dimension that is several times the square of the number of bar FEs. These advantages allow accurate solutions and the strength of the interfacial stress singularity can be correctly assessed.

2. Variational formulation

An elastic bar of length L and cross section A bonded to an elastic half-plane, as shown in Fig. 1, is considered. Reference is made to a Cartesian coordinate system (O, x, y) centred at the middle of the bar, with the vertical axis y directed toward the half-plane and the horizontal axis x placed along the interface. Both the bar and the semi-infinite substrate are considered homogeneous and isotropic solids **characterised** by linearly elastic behaviour. Small displacements and infinitesimal strains are assumed in the analysis. In the following, E_b , ν_b and α_b denote the Young modulus, the Poisson ratio and coefficient of thermal expansion of the bar, whereas E_s and ν_s represent the Young modulus and the Poisson ratio of the elastic half-space, respectively. **Generalised** plane stress or plane strain regime can be considered in the study; in the latter case, the width h of the half-plane will be assumed unitary. The thickness of the coating is assumed thin, making it possible to neglect its bending stiffness. This assumption leads to the vertical component of stress (peel stress) being ignored in the **bar**, consequently, only interfacial shear stress $t(x)$ occurs along the contact region. Moreover, perfect adhesion is **assumed** between the bar and the half-plane boundary, i.e. the extension of the contact region is known *a priori*. The system is subjected to a generically distributed horizontal load $p(x)$ and thermal variation $\Delta T(x)$.

The solutions of the elastic problem for a homogeneous isotropic half-plane loaded by a point force normal or tangential to its boundary are known as Flamant or Cerruti solutions, respectively [16,28]. In particular, the Green function $g(x, \hat{x})$ can be expressed in closed form **solution**

$$g(x, \hat{x}) = -\frac{2}{\pi E} \ln \frac{|x - \hat{x}|}{d}, \quad (1)$$

where $E = E_s$ or $E = E_s / (1 - \nu_s^2)$ for a **generalised** plane stress or plane strain state, respectively, and d represents an arbitrary length related to a rigid-body displacement. Then, the horizontal surface displacement $u(x)$ due to the interfacial tractions acting along the boundary between the half-plane and the bar can be found by integrating the Green function $g(x, \hat{x})$, **namely**

$$u(x) = \int_L g(x, \hat{x}) t(\hat{x}) d\hat{x}, \quad (2)$$

By means of the theorem of work and energy for exterior domains [29], one can demonstrate that the total potential energy Π_s for the

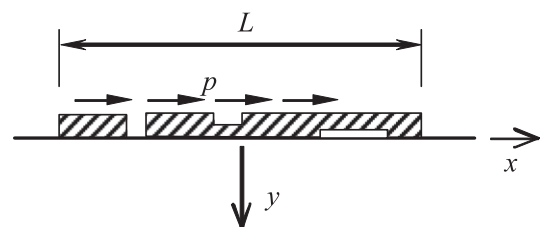


Fig. 1. Bar attached on semi-infinite substrate.

half-plane equals one half of the external work of loads [27]

$$\Pi_s = -\frac{h}{2} \int_L t(x) u(x) dx, \quad (3)$$

By introducing Eq. (2) into Eq. (3) one obtains

$$\Pi_s = -\frac{h}{2} \int_L t(x) dx \int_L g(x, \hat{x}) t(\hat{x}) d\hat{x}, \quad (4)$$

The total potential energy for the bar in terms of the mechanical and thermal components of axial strain can be written as follows [30]:

$$\Pi_b = \frac{1}{2} \int_L E_0 A(x) [u'(x) - \alpha_0 \Delta T]^2 dx - h \int_L [p(x) - t(x)] u(x) dx, \quad (5)$$

where $E_0 = E_b$, $\alpha_0 = \alpha_b$ or $E_0 = E_b / (1 - \nu_b^2)$, $\alpha_0 = (1 + \nu_b) \alpha_b$ for a generalised plane stress or plane strain state, respectively, and prime denotes differentiation with respect to x . It is worth noting that axial force in the bar is given by $N(x) = E_0 A(x) [u'(x) - \alpha_0 \Delta T]$.

Finally, the total potential energy $\Pi = \Pi_b + \Pi_s$ of the system is found to be

$$\Pi(u, t) = \frac{1}{2} \int_L E_0 A [u'(x) - \alpha_0 \Delta T]^2 dx - h \int_L [p(x) - t(x)] u(x) dx - \frac{h}{2} \int_L t(x) dx \int_L g(x, \hat{x}) t(\hat{x}) d\hat{x}, \quad (6)$$

Similar variational formulation can be found in [27], where a Timoshenko beam in frictionless contact with the underlying soil is studied. In the framework of contact problems, useful mathematical references are [33–35], where well-posedness of the variational problem and of the corresponding Galerkin solution is set in proper abstract functional framework. Nonetheless, Eq. (6) has not been previously suggested to study axially loaded bar bonded to an elastic half-plane.

3. Finite element model

Both the elastic bar and the substrate boundary are divided into finite elements. In particular, the bar is partitioned into finite elements of length l_i and a set of linear or quadratic Lagrange polynomials $N_i(\xi)$ is adopted as shape functions [36], where ξ represents the dimensionless local coordinate, i.e. $\xi = x/l_i$. As customary, nodal displacements \mathbf{q}_i characterize completely the axial displacement in each finite element by means of the vector $\mathbf{N}(\xi)$ containing the shape functions:

$$u(\xi) = [\mathbf{N}(\xi)]^T \mathbf{q}_i. \quad (7)$$

The substrate boundary underlying the bar is divided into finite elements also. It is worth noting that mesh for the surface of the half-plane can be defined independently from that of the bar. Similar to expression (7), the interfacial shear stress arising in the i th substrate element can be approximated as follows:

$$t(\xi) = [\mathbf{p}(\xi)]^T \mathbf{t}_i, \quad (8)$$

\mathbf{p} being a vector collecting the shape functions and \mathbf{t}_i represents the vector of nodal substrate tractions. In the present study, only piecewise constant functions are used to interpolate the shear tractions in Eq. (8). As shown later, this assumption will lead to accurate results.

In the following, each bar element with linear polynomials may have either one or two equal constant substrate elements of total length l_i , denoted by B1S1 or B1S2, respectively (Fig. 2a and b). Similarly, bar element with quadratic polynomials and either one or two equal constant substrate elements are denoted by B2S1 or B2S2, respectively (Fig. 2c and d).

Substituting Eqs. (7) and (8) in variational principle (6) and assembling over all the elements, the potential energy takes the

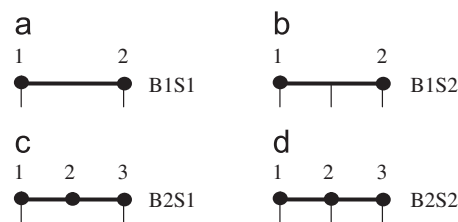


Fig. 2. Linear (a, b) and quadratic (c, d) bar elements including one (a, c) or two (b, d) equal substrate elements.

expression:

$$\Pi(\mathbf{q}, \mathbf{t}) = \frac{1}{2} \mathbf{q}^T \mathbf{K}_b \mathbf{q} - \mathbf{q}^T \mathbf{F} + \mathbf{q}^T \mathbf{H} \mathbf{t} - \frac{1}{2} \mathbf{t}^T \mathbf{G} \mathbf{t}, \quad (9)$$

where \mathbf{K}_b is the bar stiffness matrix and \mathbf{F} the external load vector, whose elements take the usual form

$$k_{ij} = l_i \int_0^1 E_0 A(\xi) N'_i(\xi) N'_j(\xi) d\xi, \quad (10)$$

$$f_i = l_i \int_0^1 (N_i(\xi) p(\xi) h + N'_i(\xi) E_0 A(\xi) \alpha_b \Delta T) d\xi, \quad (11)$$

The components of matrices \mathbf{H} and \mathbf{G} are given by the following expressions:

$$h_{ij} = h l_i \int_0^1 N_i(\xi) \rho_j(\xi) d\xi, \quad (12)$$

$$g_{ij} = h \int_{x_i}^{x_{i+1}} dx \rho_i(x) \int_{x_j}^{x_{j+1}} g(x, \hat{x}) \rho_j(\hat{x}) d\hat{x}, \quad (13)$$

where x_i, x_{i+1} are the coordinates of the i th element and element matrices of Eq. (9) are reported in the Appendix. It should be noted that, unlike the local pressure–displacement law assumed in a Winkler-type model [31,32], the present formulation takes into account the nonlocal response of the system through the fully populated matrix \mathbf{G} . Furthermore, the integral in Eq. (13) is weakly singular, i.e. always exists in the Cauchy principal value sense and is finite. The use of piecewise constant functions to interpolate the shear stress leads to a simpler analytical evaluation of components g_{ij} in Eq. (13). Moreover, it can be proved that the approximated shear stress converges to the shear stress solution in the proper functional space [37,38]. Higher-order degree interpolating functions make the analytical integration more cumbersome and numerical evaluation of a weakly singular integral needs to be considered, with an increase of computational burden. Nonetheless, for fixed number of finite elements, the use of higher-order degree interpolating functions could increase the convergence rate.

As usual, the problem can be solved by imposing the potential energy functional (9) to be stationary, leading to the following equality:

$$\begin{bmatrix} \mathbf{K}_b & \mathbf{H} \\ \mathbf{H}^T & -\mathbf{G} \end{bmatrix} \begin{Bmatrix} \mathbf{q} \\ \mathbf{t} \end{Bmatrix} = \begin{Bmatrix} \mathbf{F} \\ \mathbf{0} \end{Bmatrix}. \quad (14)$$

The solution of Eq. (14) provides the nodal displacements and tractions

$$\mathbf{t} = \mathbf{G}^{-1} \mathbf{H}^T \mathbf{q}, \quad (15)$$

$$(\mathbf{K}_b + \mathbf{K}_s) \mathbf{q} = \mathbf{F}, \quad (16)$$

\mathbf{K}_s being the stiffness matrix for the substrate.

$$\mathbf{K}_s = \mathbf{H} \mathbf{G}^{-1} \mathbf{H}^T. \quad (17)$$

In particular, Eq. (16) represents the discrete system of equations governing the response of the bar–substrate system.

In the case of a bar detached from the substrate between the nodes d_1 and d_2 , where no shear stress is transmitted, the bar stiffness matrix \mathbf{K}_b is assembled as usual and system (14) can be partitioned as follows:

$$\begin{bmatrix} \mathbf{K}_b & \mathbf{0} \\ \mathbf{H}_L^T & \mathbf{0} \end{bmatrix} \begin{bmatrix} \mathbf{q}_L \\ \mathbf{q}_d \\ \mathbf{q}_R \\ \mathbf{t} \end{bmatrix} = \begin{bmatrix} \mathbf{F}_L \\ \mathbf{F}_d \\ \mathbf{F}_R \\ \mathbf{0} \end{bmatrix} \quad (18)$$

where $\mathbf{q}_L = [q_1, \dots, q_{d1}]^T$ and $\mathbf{q}_R = [q_{d2}, \dots, q_n]^T$ are the nodal displacements at the left and right side of the detached region having nodal displacements $\mathbf{q}_d = [q_{d1}, \dots, q_{d2}]^T$ and \mathbf{F}_L , \mathbf{F}_R and \mathbf{F}_d are the corresponding external load vectors. Moreover, tractions \mathbf{t} as well as matrices \mathbf{H}_L , \mathbf{H}_R are defined in the bar FEs attached to the substrate only.

3.1. Numerical properties of the FE model

The mapping properties of the BIE (2) are well known [38–39]. In particular, a continuous, positive-definite and symmetric bilinear form is associated to the logarithmic kernel (1), whereas stability and convergence of Galerkin scheme related to Eq. (15) was verified in [38] for increasing number of piecewise functions. Consequently, \mathbf{G} and \mathbf{G}^{-1} being positive definite (i.e. $\mathbf{y}^T \mathbf{G} \mathbf{y} > 0$ and $\mathbf{y}^T \mathbf{G}^{-1} \mathbf{y} > 0$ for all nonzero \mathbf{y}), \mathbf{K}_s is also positive-definite for all \mathbf{q} , except for the special occurrence $\mathbf{H}^T \mathbf{q} = \mathbf{0}$, i.e. for \mathbf{q} belonging to the kernel of \mathbf{H}^T . In fact, by pre- and post-multiplying both sides of Eq. (17) by vectors \mathbf{q}^T and \mathbf{q} , respectively, one obtains $\mathbf{q}^T \mathbf{K}_s \mathbf{q} = \mathbf{q}^T \mathbf{H} \mathbf{G}^{-1} \mathbf{H}^T \mathbf{q} > 0$ provided that $\mathbf{y} = \mathbf{H}^T \mathbf{q}$ is a nonzero vector [40]. Moreover, \mathbf{K}_s being positive definite, the sum of $\mathbf{K}_b + \mathbf{K}_s$ in Eq. (16) remains positive-definite even with \mathbf{K}_b being positive semidefinite. In fact, $\mathbf{q}^T (\mathbf{K}_b + \mathbf{K}_s) \mathbf{q} = \mathbf{q}^T \mathbf{K}_b \mathbf{q} + \mathbf{q}^T \mathbf{K}_s \mathbf{q} > 0$ for all \mathbf{q} not belonging to the kernel of \mathbf{H}^T .

In the case of equally spaced B1S1 elements, each of which includes one substrate element, the kernel of \mathbf{H}^T contains the vector $\mathbf{q} = [1, -1, 1, -1, \dots]^T$, which gives rise to zero mean axial displacement in each element. In this case, the work done by the axial force and the constant substrate tractions is zero (see Fig. 3a), yielding spurious zero energy modes. Nonetheless, if equally spaced B1S2 elements are used (Fig. 3b), the null space of $\mathbf{H}^T = \{\mathbf{0}\}$ and \mathbf{K}_s is found to be positive-definite for all vectors \mathbf{q} .

Usually, stability and convergence of the mixed FE model may be verified by checking the behaviour of the smallest generalised singular value of \mathbf{H}^T , which is related to the inf-sup (or LBB) condition [41]. In fact, zero singular values of \mathbf{H}^T characterize the null space of \mathbf{H}^T and, in this respect, B1S1 element does not satisfy the inf-sup condition. Nonetheless, the numerical examples considered in the next section have solutions not belonging to the kernel of \mathbf{H}^T , for this reason FEs not satisfying the inf-sup condition can be used in some cases.

4. Numerical examples

In the present section, several loading cases of a bar bonded to the underlying half-plane are considered and discussed. Unless otherwise stated, a number of 512 equal B2S1 FEs are used to model the elastic bar, where a single substrate element is included in each bar element, and a proper value is imparted to the length d associated with a rigid displacement, such as to involve zero displacement at the bar end.

Similar to [1], the parameter characterising the elastic response of the bar-substrate system is taken as

$$\beta L = \frac{EhL}{E_0 A}. \quad (19)$$

Low values of βL characterise short bars stiffer than the substrate, when the bar performs like an almost inextensible stiffener. Higher values of βL describe more flexible bars, thus are appropriate for long bars bonded to stiff substrate.

4.1. Bar subject to a horizontal point force at the midpoint

The case of a bar bonded to the underlying substrate and loaded by a horizontal force of magnitude P applied at the midpoint is discussed first. In Figs. 4–6 dimensionless axial displacement $u/[P/(E_s h)]$, axial force N/P and substrate reaction $t/[P/(hL)]$ are plotted versus the dimensionless abscissa x/L , for three values of the rigidity parameter, i.e. $\beta L = 1, 10, 100$, respectively, which correspond to decreasing stiffness of the bar with respect to the substrate. In the same figures, axial force and substrate reaction corresponding to a number of 16 equal B1S1 finite elements are also reported. In this case, the axial force is piecewise constant and adequately predicts the actual distribution for $\beta L = 1$ and 10.

Fig. 4 refers to $\beta L = 1$, the bar tends to behave like an inextensible stiffener, resulting in an almost bi-linear trend of horizontal displacement, as shown by Fig. 4a. Also the axial force varies linearly and exhibits a jump in correspondence with the point of load application, whereas substrate shear reaction in the neighbourhood of the bar ends is well approximated by the analytical expression arising from the problem of inextensible stiffener [10,42]:

$$t_1(x) = \frac{2P}{\pi h L} \frac{1}{\sqrt{1 - 4(x/L)^2}} \quad (20)$$

where a singular behaviour at the bar ends is expected. This behaviour can be observed in Fig. 4c even using only 16 equally-spaced B1S1 FEs.

Conversely, for high values of βL , the effects of the longitudinal force are concentrated in the neighbourhood of the point force application, as depicted by Fig. 6. In particular, the shear tractions and horizontal displacement assume low values along the entire bar, except around the application of the point force. In this case,

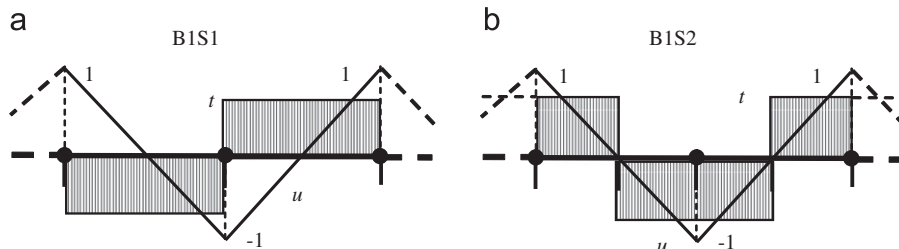


Fig. 3. Linear bar elements including one (a) or two (b) equal substrate elements characterised by nodal displacements $\mathbf{q} = [1, -1, 1, -1, \dots]^T$ and piecewise constant interfacial stress.

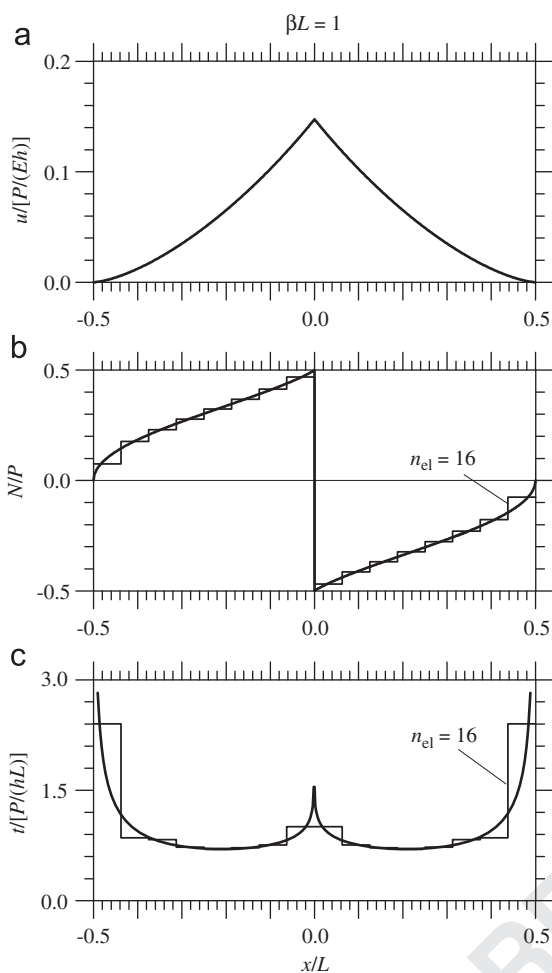


Fig. 4. Bar loaded by a concentrated force at the midpoint. Axial displacement (a), axial force (b) and substrate reaction (c) along the bar for $\beta L = 1$.

16 equal B1S1 FEs are unable to predict adequately the bar midpoint reaction, as shown in Fig. 6c.

In the neighbourhood of the point load, Melan solution is a good approximation [1,5]

$$N_2(x) = \frac{P}{\pi} \left[\text{si} \left(\frac{\beta x}{2} \right) \cos \left(\frac{\beta x}{2} \right) - \text{ci} \left(\frac{\beta x}{2} \right) \sin \left(\frac{\beta x}{2} \right) \right] \quad (21)$$

$$t_2(x) = -\frac{P \beta}{h 2\pi} \left[\text{ci} \left(\frac{\beta x}{2} \right) \cos \left(\frac{\beta x}{2} \right) + \text{si} \left(\frac{\beta x}{2} \right) \sin \left(\frac{\beta x}{2} \right) \right] \quad (22)$$

where si and ci denote sine and cosine integrals, respectively. The interfacial shear stress in the neighbourhood of the bar midpoint and bar end is reported in Fig. 7. In order to compare the results obtained by the proposed model with analytical solutions, a suitable mesh refinement is implemented by means of 202 logarithmically spaced B2S1 FEs. In particular, with reference to the positive axis only and disregarding the B2S1 FE internal points, a number of 37 logarithmically spaced points are generated in the interval $[10^{-5}, 0.1]/L$, 10 logarithmically spaced points in the interval $[0.1, 0.4]/L$ and 55 logarithmically spaced points in $[0.4, 0.5 - 10^{-7}]/L$.

In Fig. 7a, the shear stress in the neighbourhood of the point load is plotted in dimensionless form versus βx . As x tends to zero, Melan solution reported in Eq. (22) reduces to

$$\lim_{x \rightarrow 0} t_2(x) = -\frac{P \beta}{h 2\pi} \left[\gamma + \log \left(\frac{\beta x}{2} \right) \right] \quad (23)$$

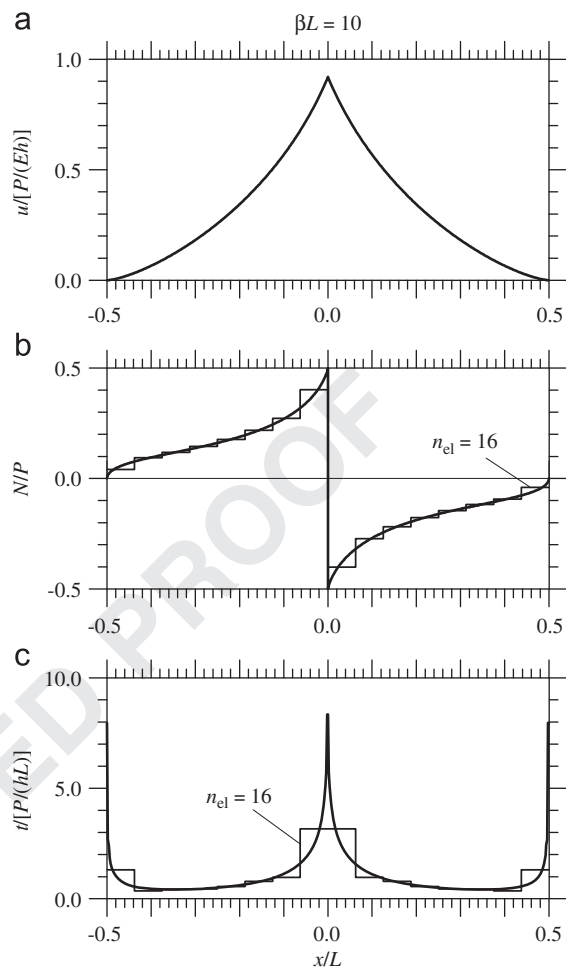


Fig. 5. Bar loaded by a concentrated force at the midpoint. Axial displacement (a), axial force (b) and substrate reaction (c) along the bar for $\beta L = 10$.

where γ is the Euler constant, with numerical value approximately equal to 0.5772. As shown in Fig. 7a, the Melan solution is retrieved for $\beta L \geq 5$. Moreover, the curves of the interfacial shear stress for different values of βL are characterised by almost the same slope. Therefore, logarithmic singularity occurs for all values of the bar-substrate parameter. For $\beta L = 1$, the Euler constant in Eq. (23) has to be replaced with numerical value approximately equal to -1.6 . Note that the curve related to the shear stress for $\beta L = 5$ is below those concerning the shear stress for $\beta L = 1$, since the dimensionless shear tractions are normalised with respect to the parameter βL .

Fig. 7b shows (in logarithmic scale) the dimensionless shear stress versus x/L in the neighbourhood of the bar end. For $\beta L = 1$, interfacial shear stress is well approximated by Eq. (20) related to the inextensible stiffener. Moreover, a square-root singularity also occurs for $\beta L = 10$ and 100, but with different strengths of singularity.

4.2. Shear stress singularity factor K_{II} for some load conditions

The strength of singularity of the interfacial stress in the neighbourhood of the bar end $x/L = 0.5$ can be investigated by means of the shear stress singularity factor K_{II} , typically defined as [43]

$$K_{II} = \lim_{x \rightarrow L/2} \sqrt{2\pi(L/2 - x)} t(x) \quad (24)$$

From a numerical point of view, the function on the right hand side of Eq. (24) is evaluated at various locations x/L , the value

located at $10^{-6}/L$ from the end is the sought value of K_{II} . The interval $[0.5 - 10^{-7}, 0.5]/L$ is disregarded since large oscillations in interfacial stress occur. For a bar loaded by a horizontal point force at the middle, the values of K_{II} evaluated in the neighbourhood of the bar end $x/L=0.5$ may be smaller than those evaluated at the middle through Eq. (24). Indeed, K_{II} tends to infinity for $x=0$ because of the logarithmic singularity occurring at the midpoint. In this case, Eq. (24) is a nonmonotonic function of x .

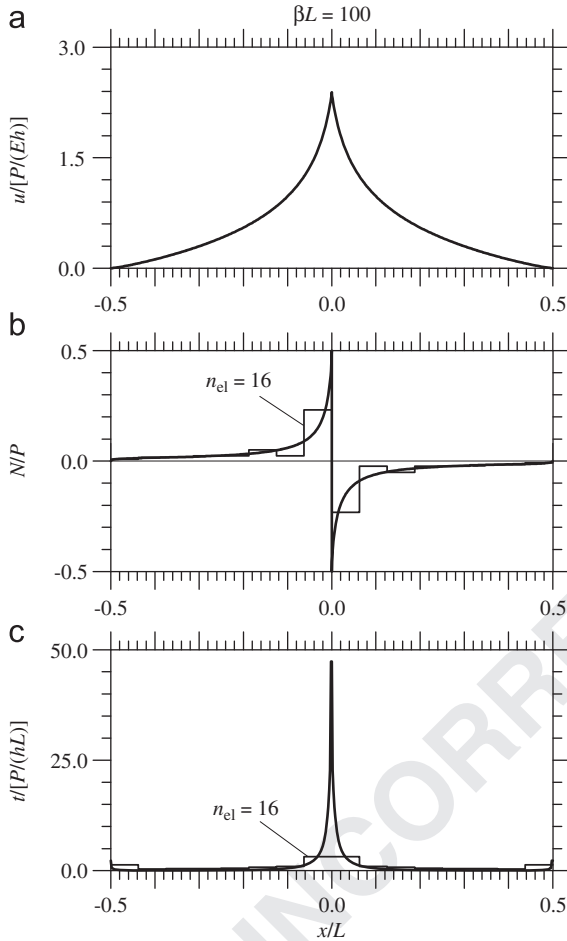


Fig. 6. Bar loaded by a concentrated force at the midpoint. Axial displacement (a), axial force (b) and substrate reaction (c) along the bar for $\beta L=100$.

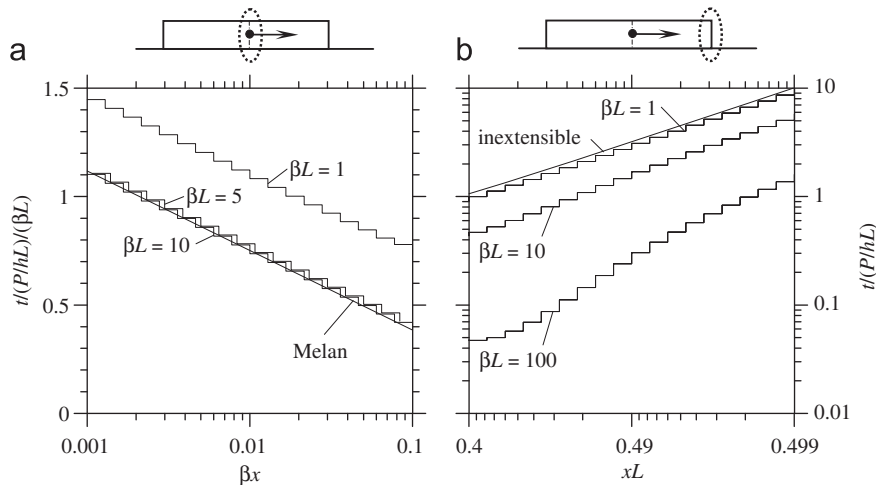


Fig. 7. Bar loaded by a concentrated force at the midpoint. Substrate reaction in the neighbourhood of the bar midpoint (a) and bar end (b).

Fig. 8 shows the K_{II} factor, in dimensionless form, versus $1/2 - x/L$ for a bar loaded by a horizontal point force at the middle and at the bar end, for some values of the parameter βL . As reported in Fig. 8a, for a bar loaded by a point force at the midpoint, the K_{II} factor in the neighbourhood of the bar end decreases as βL increases, confirming the fact that the strength of the interfacial stress singularity diminishes for compliant bars. Indeed, the largest value of the strength singularity is reached for an inextensible bar, for which Eq. (20) yields

$$K_{II} = \sqrt{\frac{2}{\pi}} \frac{P}{h\sqrt{L}} = 0.7979 \frac{P}{h\sqrt{L}} \quad \text{for } \beta L \rightarrow 0 \quad (25)$$

Conversely, for a bar loaded at its right end by a tangential point force, the K_{II} factor increases with the compliance of the bar, being the smallest value of K_{II} attained for an inextensible bar, as shown in Fig. 8b. This behaviour is reflected in Fig. 9, which depicts the values of the K_{II} factor in the neighbourhood of the bar end, varying the rigidity parameter βL for different load conditions. As expected, for a very stiff bar ($\beta L \rightarrow 0$), the strength of singularity is weakly sensitive to the position in which the load is applied, as shown by the curve of Fig. 8b for an inextensible bar, for which the K_{II} factor is almost constant along the bar. Nonetheless, even for small values of βL , the K_{II} factor significantly depends on the stiffness and the load position. This confirms that the interfacial stress tends to concentrate in correspondence with the point of load application, particularly for compliant bars. Moreover, for P in $x/L=1/2$, the K_{II} parameter agrees well with that calculated by Koiter [7] who studied a semi-infinite bar bonded to a half-plane and loaded by a point force at its end, which can be evaluated as follows [15]:

$$K_{II,Koiter} = \sqrt{\beta} \frac{P}{h} = \sqrt{\beta L} \frac{P}{h\sqrt{L}} \quad (26)$$

In particular, for $\beta L > 4$, Eq. (26) differs from the K_{II} factor by less than 3%. It should be noted that, for some special values of x/L (e.g. P in $x/L=0.4$), the K_{II} parameter is not monotonic increasing with βL .

4.3. Axial force for the bar subject to a horizontal point force at the midpoint or at the end

The dimensionless axial force versus βx for a bar loaded by a concentrated force at the midpoint is reported in Fig. 10a for some values of βL . The numerical results agree well with Melan solution for $\beta L=100$, i.e. for a sufficiently compliant bar with respect to the underlying substrate. Nonetheless, Melan solution is well

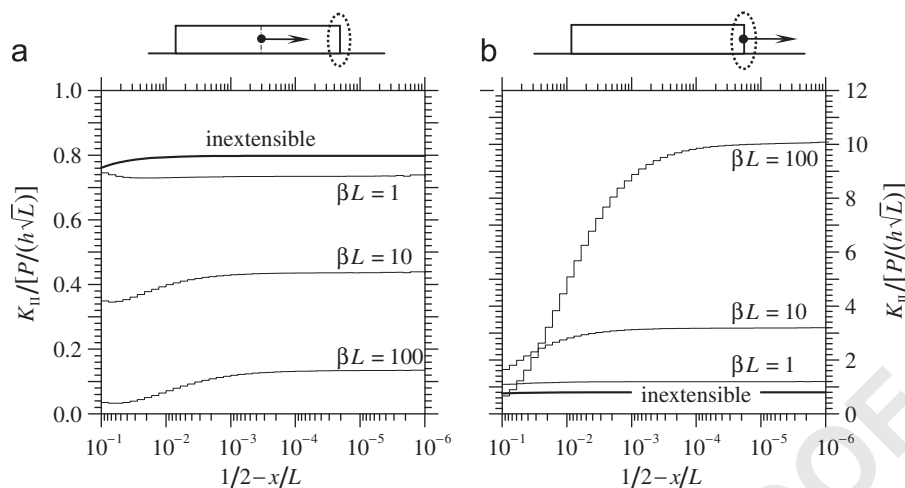


Fig. 8. Shear Stress Singularity Factor K_{II} in the neighbourhood of bar end $x/L=0.50$. Bar loaded by a concentrated force at the midpoint (a) and at the bar end (b).

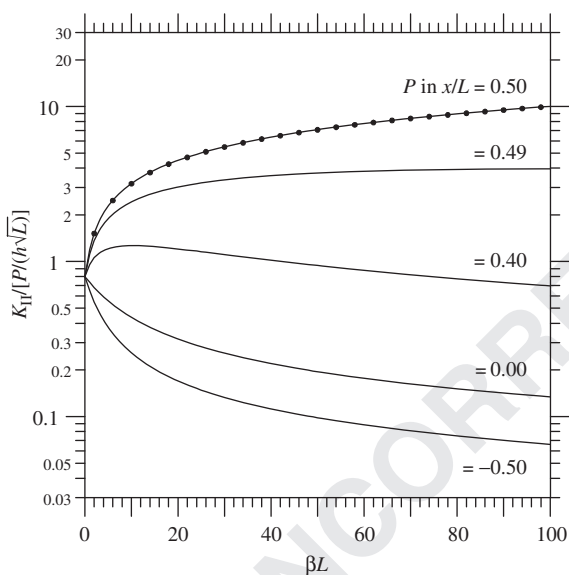


Fig. 9. Shear Stress Singularity Factor K_{II} in the neighbourhood of bar end $x/L=0.50$ versus βL for bar loaded by a concentrated force at $x/L=0.50$, 0.49, 0.40, 0.0, -0.50.

retrieved for lower values of βL also, i.e. for $\beta L > 5$ provided that $\beta x < 1/2$. Moreover, the dimensionless axial force versus $\beta L/2 - \beta x$ for a bar loaded by a concentrated force at the end is reported in Fig. 10b. The curve related to $\beta L \geq 10$ practically coincides with the Koiter solution, even if a large agreement with respect to this classical solution can be observed for $\beta L \geq 5$ if $\beta(L/2 - x) < 1$. For rigid bars (e.g. $\beta L=1$), the axial force along the bar tends to a linear trend, as shown by Fig. 4b.

4.4. Bar subject to uniform thermal load

The case of an elastic bar loaded by a uniform thermal variation ΔT is similar to that of a bar symmetrically loaded by two opposite forces applied at the ends (see Fig. 11). In particular, the axial displacement and the interfacial shear stress of a bar subject to a uniform thermal load ΔT coincide with those induced in the bar by two opposite axial forces of magnitude $\Theta = E_0 \alpha_0 \Delta T$ applied at the ends [15]. As for the discrete problem and

assuming consecutive bar FEs, the vector of equivalent external loads reduces to $\mathbf{F} = \Theta [-1, 0, \dots, 0, 1]^T$ (see Appendix). The axial force of a bar subject to two opposite forces Θ equals that of the same bar subject to a thermal load ΔT increased by the quantity $E_0 \alpha_0 \Delta T$. Moreover, the stress intensity factors in the neighbourhood of the ends of a bar under thermal load, $K_{II}(\Delta T)$, can be obtained by properly superposing the K_{II} factors of a bar subject to two opposite forces of magnitude Θ . For example, $K_{II}(\Delta T)$ in $x/L=0.5$ can be evaluated as K_{II} related to an axial force of magnitude Θ acting at $x/L=0.5$ plus K_{II} related to an axial force of magnitude $-\Theta$ acting at $x/L=-0.5$, i.e. $K_{II}(\Delta T, x/L=0.5) = K_{II}(\Theta, x/L=0.5) + K_{II}(-\Theta, x/L=-0.5)$.

4.5. Detached bar

Some results concerning a bar detached bar between $x/L=0.30$ and $x/L=0.40$ are reported in Figs. 12–15. For a bar with $\beta L=10$ and loaded by a point force applied at the bar end, dimensionless axial displacement, axial force and interfacial stress are depicted in Fig. 12a–c, respectively. As expected, constant axial force and zero substrate reaction are found inside the detached region. Apart from the neighbourhood of the detached region, the results related to the detached bar are almost identical to those of the fully bonded bar.

A number of 261 logarithmically spaced B2S1 FEs are used. In particular, disregarding the B2S1 FE internal nodes, a number of 55 logarithmically spaced points are generated in the intervals $[-0.5 + 10^{-7}, -0.4]/L$, $[0.2, 0.3 - 10^{-7}]/L$, $[0.4 + 10^{-7}, 0.45]/L$ and $[0.45, 0.5 - 10^{-7}]/L$, where stress singularity is expected. At the ends of the detached region, the shear stress singularity factors K_{II} are defined as

$$K_{II}(0.3L) = \lim_{x \rightarrow 0.3L} \sqrt{2\pi(0.3L-x)t(x)} \quad (27)$$

$$K_{II}(0.4L) = \lim_{x \rightarrow 0.4L} \sqrt{2\pi(x-0.4L)t(x)} \quad (28)$$

Similar to Fig. 8, Fig. 13 shows the shear stress singularity factor K_{II} for the detached bar loaded by a concentrated force P applied at the bar end for some values of βL . As reported in Fig. 13a and excluding the case of an inextensible bar, the K_{II} parameters in the neighbourhood of $x/L=0.4$ are smaller than the same quantities evaluated near the bar end (Fig. 13b). Moreover, as shown by Figs. 13b and 14, the K_{II} factors in the neighbourhood

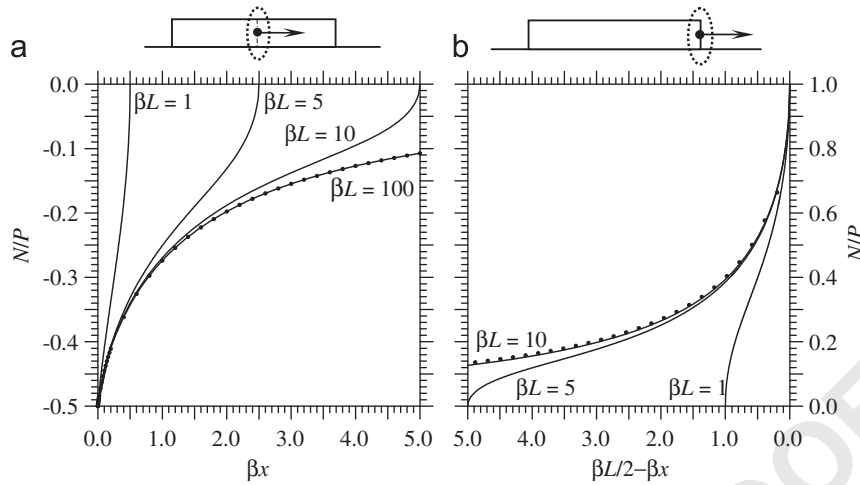


Fig. 10. Axial force versus βx for a bar loaded by a concentrated force at the midpoint (a) and axial force versus $\beta(L/2 - x)$ for a concentrated force P applied at the bar end $x/L=0.50$ (b).

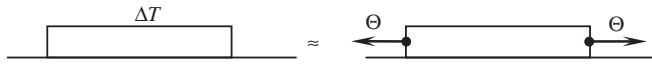


Fig. 11. Sketch of a bar loaded by a uniform thermal variation. This load situation is similar to two opposite axial forces of magnitude $\Theta = E_0 A \alpha_0 \Delta T$ applied at the ends of the bar.

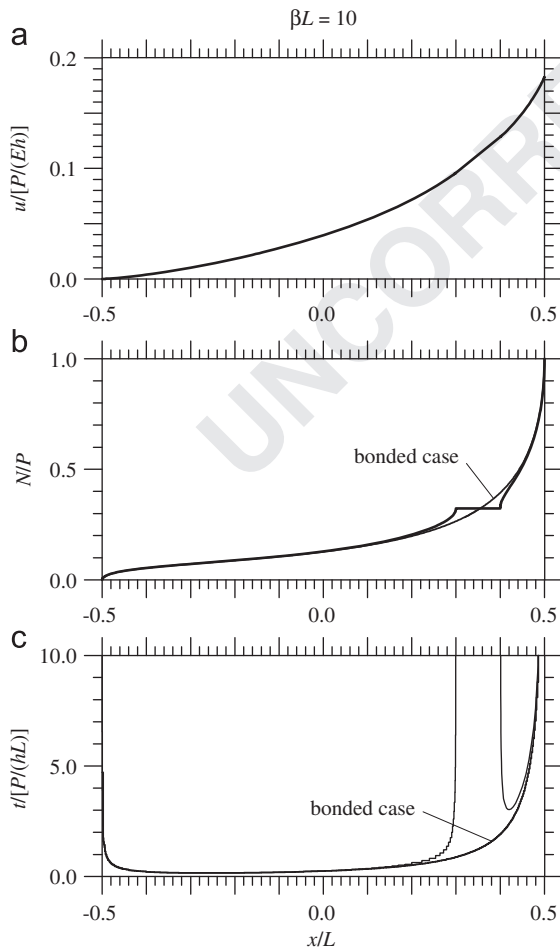


Fig. 12. Bar loaded by a concentrated force P applied at the bar end $x/L=0.50$ and detached between $x/L=0.30$ and $x/L=0.40$. Axial displacement (a), axial force (b) and substrate reaction (c) along the bar for $\beta L=10$.

of the bar end are slightly greater than the corresponding K_{II} factors of a perfectly bonded bar.

For a bar with $\beta L=10$, dimensionless axial displacement, axial force and substrate reaction of a detached bar subject to a constant thermal variation ΔT are reported in Figs. 15a–c, respectively. As expected, the maximum amplitude of horizontal displacement occurs at the end of the bar, whereas the axial force attains the largest magnitude in the middle. Small differences are found with respect to the solution of the bonded bar, except in the neighbourhood of the detached region.

5. Conclusions

A coupled FE–BIE method has been proposed to evaluate the mechanical behaviour of elastic thin structures bonded to a homogeneous isotropic half-plane under axial forces or thermal loads. Plane strain or generalised plane stress regime of the bar–substrate system has been considered in the present study. Bar FEs have been used to simulate the bonded structures, whereas the behaviour of the semi-infinite substrate has been represented through BIE only. A mixed variational formulation involving the Green function of the half-plane has been used, providing a proper relation between the axial displacement and the interfacial stress. The proposed method has been utilised to study in detail the contact problem of an elastic bar bonded to a half-plane. The evaluation of the strength of the stress singularities occurring at the ends of the contact region and in the neighbourhood of the point of load application has been given in terms of shear stress singularity factors. Various loading conditions of the bar have been investigated, including the case of a bar partially detached from the substrate. The rigidity parameter βL , representing the stiffness of the bonded bar with respect to the half-plane, is found to characterize the mechanical response of the system. In particular, for a bar loaded at the midpoint by an axial force, a large agreement among the obtained results with the Melan solution is found for $\beta L \geq 100$, i.e. for a sufficiently compliant bar with respect to the underlying substrate. In fact, a substantial agreement with respect to the Melan solution is also found for lower values of βL in the neighbourhood of load application. Moreover, for $\beta L=1$ (rigid bar), the substrate reaction provided by the analytical solution of the contact problem for an inextensible bar is retrieved. For a bar axially loaded at the end, the comparison of the obtained results with the Koiter solution is given, establishing a large agreement for $\beta L \geq 10$. A good

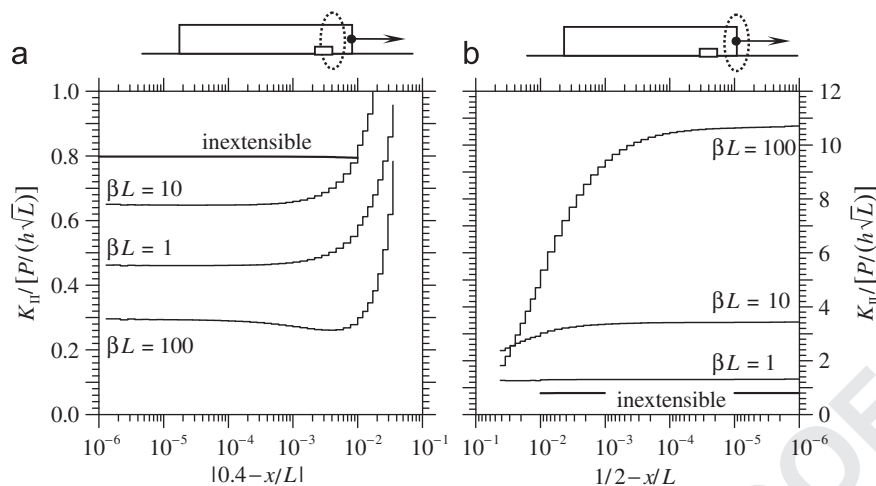


Fig. 13. Detached bar loaded by a concentrated force P applied at the bar end. Shear Stress Singularity Factor K_{II} in the neighbourhood of $x/L=0.4$ (a) and bar end $x/L=0.5$ (b).

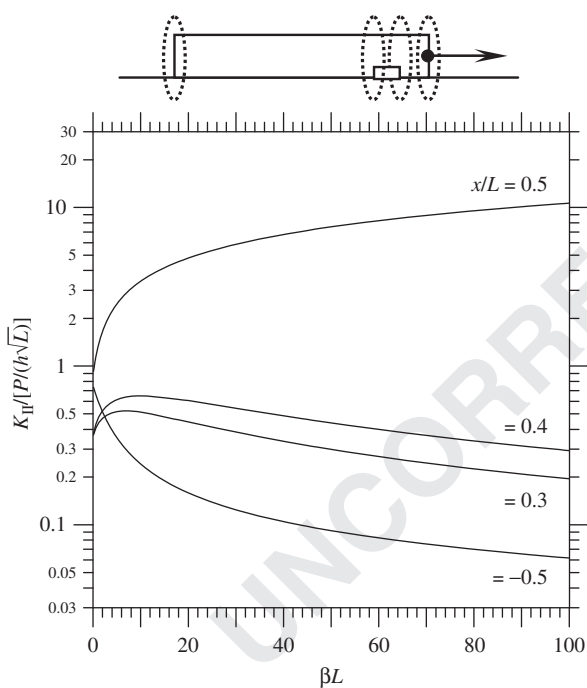


Fig. 14. Detached bar loaded by a concentrated force P applied at the bar end. Shear Stress Singularity Factors K_{II} versus βL for $x/L=0.50, 0.40, 0.30, -0.50$.

agreement is also found for $\beta L \geq 5$ in the neighbourhood of the bar end. In both cases, the shear stress is found to be concentrated in correspondence with the point of load application, particularly for compliant bars. The case of bars loaded by a uniform thermal variation is also discussed, establishing similarity with respect to the problem of a bar loaded at the ends by two opposite axial forces. Finally, a detached bar loaded by an axial force at an end or by a thermal load is considered, establishing almost the same results of a completely welded bar, except in the region close to the detached zone. Nonetheless, the shear stress singularity factors evaluated in the neighbourhood of the bar end are smaller than those related to a perfectly bonded bar due to the fact that the interior detachment diminishes the length of the bonded region, resulting in increasing of the stiffness of the bonded portions of the bar.

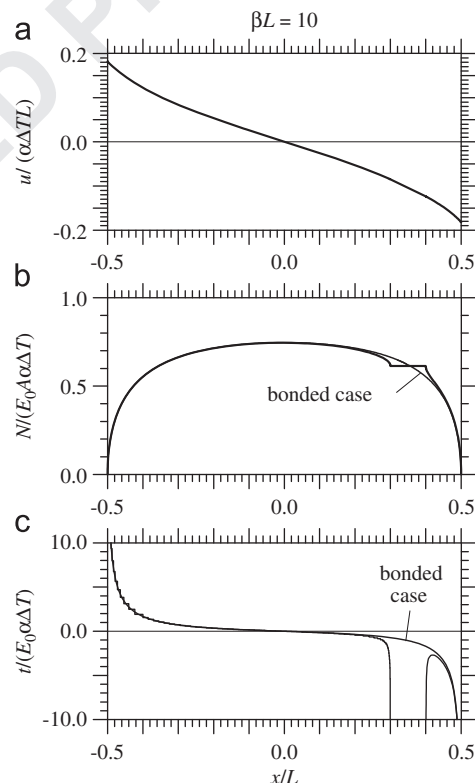


Fig. 15. Bar subject to a thermal variation $-\Delta T$ and detached between $x/L=0.30$ and $x/L=0.40$. Axial displacement (a), axial force (b) and substrate reaction (c) along the bar for $\beta L=10$.

Acknowledgements

The present investigation was developed in the framework of the two Italian Research Programs no. 2007YZ3B24 (coordinated by Prof. Alberto Corigliano from the Polytechnic of Milan) and no. 20089RJKN (coordinated by Prof. Franco Maceri of University of Rome "Tor Vergata"), the Research Program FAR 2009 of the University of Ferrara, and the Research Program funded by the Italian Civil Protection National Service—Executive Project 2010–2013 within the activities of the (Italian) University Network of Seismic Engineering Laboratories-ReLUIS. The financial support of

the Italian Ministry for University and Research, the University of Ferrara and ReLUIS is gratefully acknowledged.

Appendix

In the following a prismatic bar element subjected to uniform loads p and with a constant substrate pressure is considered. In the case of Lagrange linear functions $N_1 = 1 - \xi$ and $N_2 = \xi$, element matrices appearing in Eq. (9) become

$$\mathbf{K}_{bi} = \frac{E_0 A}{l_i} \begin{bmatrix} 1 & -1 \\ -1 & 1 \end{bmatrix},$$

$$\mathbf{F}_i = phl_i/2[1, 1]^T + E_0 A \alpha_0 \Delta T[-1, 1]^T,$$

$$\mathbf{H}_i = hl_i/2[1, 1]^T,$$

for the i th bar element including one substrate element,

$$\mathbf{H}_i = \frac{hl_i}{8} \begin{bmatrix} 3 & 1 \\ 1 & 3 \end{bmatrix},$$

for the i th bar element including two equal substrate elements.

In the case of Lagrange quadratic functions $N_1 = 1 - 3\xi + 2\xi^2$, $N_2 = 4\xi(1 - \xi)$ and $N_3 = \xi(2\xi - 1)$, element matrices appearing in Eq. (9) become

$$\mathbf{K}_{bi} = \frac{E_0 A}{3l_i} \begin{bmatrix} 7 & -8 & 1 \\ -8 & 16 & -8 \\ 1 & -8 & 7 \end{bmatrix},$$

$$\mathbf{F}_i = phl_i/6[1, 4, 1]^T + E_0 A \alpha_b \Delta T[-1, 0, 1]^T,$$

$$\mathbf{H}_i = hl_i/6[1, 4, 1]^T,$$

for the i th bar element including one substrate element,

$$\mathbf{H}_i = \frac{hl_i}{24} \begin{bmatrix} 5 & -1 \\ 8 & 8 \\ -1 & 5 \end{bmatrix},$$

for the i th bar element including two equal substrate elements.

Finally, components of matrix \mathbf{G} are as follows:

$$g_{ii} = \frac{2h}{\pi E} l_i^2 \left(\frac{3}{2} + \ln \frac{d}{l_i} \right),$$

$$g_{ij} = \frac{2h}{\pi E} \left[l_i l_j \left(\frac{3}{2} + \ln d \right) + G(x_{j+1} - x_{i+1}) - G(x_{j+1} - x_i) - G(x_j - x_{i+1}) + G(x_j - x_i) \right]$$

for $i \neq j$.

where $G(x) = x^2/2 \ln|x|$.

References

- [1] E.I. Grigolyuk, V.M. Tolkachev, Contact Problems in the Theory of Plates and Shells, Mir Publishers, Moscow, 1987.
- [2] L.C. Bank, Composites for Construction: Structural Design with FRP Materials, Wiley, Hoboken, New Jersey, 2006.
- [3] D.C. Agrawal, R. Raj, Measurement of the ultimate shear strength of a metal ceramic interface, Acta Metall. 37 (4) (1989) 1265–1270.
- [4] Y.L. Shen, Constrained Deformation of Materials: Devices, Heterogeneous Structures and Thermo-Mechanical Modeling, Springer, New York, 2010.
- [5] E. Melan, Der Spannungszustand der durch eine Einzelkraft im Innern beanspruchten Halbscheibe, ZAMM—J. Appl. Math. Mech./Z. Angew. Math. Mech. 12 (6) (1932) 343–346.
- [6] E.L. Buell, On the distribution of plane stress in a semi-infinite plate with partially stiffened edge, J. Math. Phys. 26 (4) (1948) 223–233.
- [7] W.T. Koiter, On the diffusion of load from a stiffener into a sheet, Q. J. Mech. Appl. Math. 8 (2) (1955) 164–178.

- [8] N.Kh. Arutiunian, Contact problem for a half-plane with elastic reinforcement, J. Appl. Math. Mech. (PMM) 32 (4) (1968) 632–646.
- [9] G.A. Morar, Gla. Popov, On a contact problem for a half-plane with elastic coverings, J. Appl. Math. Mech. (PMM) 35 (1) (1971) 172–178.
- [10] F. Erdogan, G.D. Gupta, The problem of an elastic stiffener bonded to a half plane, ASME J. Appl. Mech. 38 (4) (1971) 937–941.
- [11] S.M. Hu, Film-edge-induced stress in substrates, J. Appl. Phys. 50 (7) (1979) 4661–4666.
- [12] B.E. Alaca, M.T.A. Saif, H. Sehitoglu, On the interface debond at the edge of a thin film on a thick substrate, Acta Mater. 50 (5) (2002) 1197–1209.
- [13] X.C. Zhang, B.S. Xu, H.D. Wang, Y.X. Wu, Analytical modeling of edge effects on the residual stresses within the film/substrate systems. I. Interfacial stresses, J. Appl. Phys. 100 (11) (2006) 113524-1–113524-9.
- [14] S. Nekkanty, M.E. Walter, R. Shivpuri, A cohesive zone finite element approach to model tensile cracks in thin film coatings, J. Mech. Mater. Struct. 2 (7) (2007) 1231–1247.
- [15] L. Lanzoni, Analysis of stress singularities in thin coatings bonded to a semi-infinite elastic substrate, Int. J. Solids Struct. 48 (13) (2011) 1915–1926.
- [16] M.L. Kachanov, B. Shafiro, I. Tsukrov, Handbook of Elasticity Solutions, Kluwer Academic Publishers, Dordrecht, 2003.
- [17] M.D. Drory, M.D. Thouless, A.G. Evans, On the decohesion of residually stressed thin films, Acta Metall. 36 (8) (1988) 2019–2028.
- [18] H. Djabella, R.D. Arnell, Finite element comparative study of elastic stresses in single, double layer and multilayered coated systems, Thin Solid Films 235 (1–2) (1993) 156–162.
- [19] H. Djabella, R.D. Arnell, Two-dimensional finite-element analysis of elastic stresses in double-layer systems under combined surface normal and tangential loads, Thin Solid Films 226 (1) (1993) 65–73.
- [20] H. Djabella, R.D. Arnell, Finite element analysis of elastic stresses in multilayered systems, Thin Solid Films 245 (1–2) (1994) 27–33.
- [21] S.C. Jain, A.H. Harker, A. Atkinson, K. Pinardi, Edge-induced stress and strain in stripe films and substrates: a two-dimensional finite element calculation, J. Appl. Phys. 78 (3) (1995) 1630–1637.
- [22] J.F. Luo, Y.J. Liu, E.J. Berger, Analysis of two-dimensional thin structures (from micro- to nano-scales) using the boundary element method, Comput. Mech. 22 (5) (1998) 404–412.
- [23] Y.J. Liu, Analysis of shell-like structures by the boundary element method based on 3-D elasticity: formulation and verification, Int. J. Numer. Methods Eng. 41 (3) (1998) 541–558.
- [24] J.F. Luo, Y.J. Liu, E.J. Berger, Interfacial stress analysis for multi-coating systems using an advanced boundary element method, Comput. Mech. 24 (8) (2000) 448–455.
- [25] M. Takahashi, Y. Shibuya, Numerical analysis of interfacial stress and stress singularity between thin films and substrates, Mech. Res. Commun. 24 (6) (1997) 597–602.
- [26] M. Takahashi, Y. Shibuya, Thermoelastic analysis of interfacial stress and stress singularity between a thin film and its substrate, J. Therm. Stresses 26 (10) (2003) 963–976.
- [27] N. Tullini, A. Tralli, Static analysis of Timoshenko beam resting on elastic half-plane based on the coupling of locking-free finite elements and boundary integral, Comput. Mech. 45 (2–3) (2010) 211–225.
- [28] K.L. Johnson, Contact Mechanics, University Press, Cambridge, 1985.
- [29] M.E. Gurtin, E. Sternberg, Theorems in linear elastostatics for exterior domains, Arch. Ration. Mech. Anal. 8 (1) (1961) 99–119.
- [30] B. Szabó, I. Babuška, Finite Element Analysis, John Wiley and Sons, New York, 1991.
- [31] M. Hetenyi, Beams on Elastic Foundation, The University of Michigan Press, 1946.
- [32] B. Ferracuti, M. Savoia, C. Mazzotti, A numerical model for FRP–concrete delamination, Compos. Part B—Eng. 37 (4–5) (2006) 356–364.
- [33] N. Kikuchi, Beam bending problems on a Pasternak foundation using reciprocal variational-inequalities, Q. Appl. Math. 38 (1) (1980) 91–108.
- [34] J. Bielak, E. Stephan, A modified Galerkin procedure for bending of beams on elastic foundations, SIAM J. Sci. Stat. Comput. 4 (2) (1983) 340–352.
- [35] N. Kikuchi, J. Oden, Contact Problems in Elasticity: A Study of Variational Inequalities and Finite Element Methods, SIAM, Philadelphia, 1988.
- [36] Y.C. Fung, P. Tong, Classical and Computational Solids Mechanics, World Scientific Pub., Singapore, 2001.
- [37] S. Allinea, A. Tralli, C. Alessandri, Boundary variational formulations and numerical solution techniques for unilateral contact problems, Comput. Mech. 6 (4) (1990) 247–257.
- [38] G.C. Hsiao, W.L. Wendland, A finite element method for some integral equations of the first kind, J. Math. Anal. Appl. 58 (3) (1977) 449–481.
- [39] M. Costabel, Boundary integral operators on Lipschitz domains: elementary results, SIAM J. Math. Anal. 19 (3) (1988) 613–626.
- [40] R.A. Horn, C.R. Johnson, Matrix Analysis, Cambridge University Press, New York, 1985.
- [41] F. Brezzi, M. Fortin, Mixed and Hybrid Finite Element Methods, Springer, New York, 1991.
- [42] N.I. Muskhelishvili, Singular Integral Equation, Noordhoff, Groningen, 1953.
- [43] D. Broek, The Practical Use of Fracture Mechanics, Kluwer, Dordrecht, 1988.